



# Comparison of achromatic doublet on glass Fresnel lenses for concentrator photovoltaics

GUIDO VALLEROTTO,<sup>1,\*</sup> MARTA VICTORIA,<sup>1,2</sup> NORMAN JOST,<sup>1</sup>  
STEPHEN ASKINS,<sup>1</sup> CÉSAR DOMÍNGUEZ,<sup>1</sup> REBECA HERRERO,<sup>1</sup> AND  
IGNACIO ANTÓN<sup>1</sup>

<sup>1</sup>*Instituto de Energía Solar - Universidad Politécnica de Madrid, Avenida Complutense 30, Ciudad Universitaria, 28040, Madrid, Spain*

<sup>2</sup>*Department of Mechanical and Production Engineering - Aarhus University, Inge Lehmanns, 10 8000, Aarhus, Denmark*

\*[guido.vallerotto@upm.es](mailto:guido.vallerotto@upm.es)

**Abstract:** Silicone on glass (SoG) Fresnel lenses are the reference technology in concentrator photovoltaics (CPV) because of their simplicity and low cost. Nevertheless, their performance is strongly limited by chromatic aberration. As an alternative, in order to overcome such limitation, achromatic doublet on glass (ADG) Fresnel lenses were proposed. Such lenses are achromatic cemented doublet specifically designed for CPV applications. In this paper, a novel ADG architecture is presented and its performance analyzed and compared to previous proposals. The results show that most of the intrinsic optical losses are minimized and a superior optical efficiency can be achieved. The novel ADG design provides an achromatic lens for CPV whose efficiency is almost equal to the reference SoG technology and, at the same time, maintains all the advantages provided by the achromatic design such as the higher maximum attainable concentration and the strongly reduced temperature dependency.

© 2021 Optical Society of America under the terms of the [OSA Open Access Publishing Agreement](#)

## 1. Introduction

High concentrator photovoltaic (HCPV) has demonstrated unrivaled high photovoltaic [1,2] efficiencies in recent years based on high efficiency multi-junction (MJ) solar cell coupled with cost-effective optics used to reduce the expensive semiconductor area. The MJ solar cells are nowadays the most efficient photovoltaic devices. A six-junctions (6J) device, developed at the National Renewable Energy Laboratory (NREL), achieved recently a world record efficiency of 47.1% [3,4]. However, MJ solar cells are manufactured using expensive semiconductor materials. Thus, in order to achieve a competitive levelized cost of electricity (LCOE), the use of cheap optics to concentrate the light onto the solar cell is mandatory.

Nowadays, most of the commercially available CPV systems use Fresnel lenses as primary optical element (POE) because of their high transmittance, reduced material consumption, and high manufacturing tolerances [5,6]. Usually, Fresnel lenses are manufactured either by plastic injection of poly-methyl meta-acrylate (PMMA) or by lamination of poly-dimethyl siloxane (PDMS) over a low-iron glass rigid substrate. This last, known as silicone on glass (SoG) Fresnel lens [7], became the standard CPV technology because of its outstanding optical behavior, the ease of the manufacturing process and their proved outdoor reliability.

CPV optics have two main figures of merits: *optical efficiency* and *maximum attainable concentration*. The first is commonly defined as the fraction of radiant flux impinging at the aperture area of the optical system which reaches a designated receiver area [8–10], while the second is defined as the ratio between the optical aperture of the optics and the area of the light spot cast by the optics at its focus [8–10]. Therefore, the higher the maximum attainable concentration the smaller the solar cells to be used for the same transmitted radiant power.

The maximum attainable concentration in optical refractive systems is strongly limited by the chromatic aberration phenomenon [11] which is caused by the variation of materials refractive index as a function of the incident light wavelength. In order to enhance the maximum concentration and, at the same time, to smooth the spectral distribution of the light on the solar cell, secondary optical elements (SOE) are commonly employed [12]. Despite there are different types of SOE with different properties, all of them contribute to increase tolerance to assembly errors, tracking errors, and to reduce the thermal sensitivity of the system.

As an alternative to a SOE, the chromatic aberration can be reduced by using the so-called *achromatic doublet* [13], which is a lens composed of two individual lenses made of materials with different dispersion. An achromatic doublet provides a smaller light spot and a highly uniform light distribution without the need of any SOE. Achromatic doublets have been used in the photographic industry for a long time with the objective of reducing the chromatic aberration in the visible and near infra-red (NIR) spectrum. Unfortunately, the used materials, flint (high dispersion) and crown (low dispersion) glasses, and involved manufacturing processes are too expensive to be used in the CPV industry.

Languy and co-workers proposed an achromatic doublet for CPV composed of two plastics: PMMA and polycarbonate (PC) [14–16]. They carried out an analysis comparing different configurations of the proposed achromatic Fresnel doublet with a conventional Fresnel lens made out of PMMA. The advantages from the point of view of the maximum attainable concentration were clearly demonstrated. However, in Languy's work there is no mention to a practical manufacturing process that could be low-cost and highly scalable and, furthermore, no absolute efficiency values are disclosed, limiting the usefulness of the results.

The authors of this paper, in previous works, took a step forward presenting the achromatic doublet on glass (ADG) concept, which consists in a feasible low-cost scalable manufacturing process merging the advantages of the SoG technology and the achromatic doublet theory [17,18]. The ADG concept is based on the lamination of the doublet over a rigid solar glass, using the same process and equipment of the flat PV industry. The proposed ADG consists of an elastomer with low dispersion, a rigid plastic with high dispersion, and a rigid substrate (glass or plastic). The plastic piece operates as a mold, shaping the geometry of the elastomeric lens. The elastomer can be ethylene-vinyl acetate (EVA) or another cheap encapsulant material used in flat PV modules. The latter acts as well as glue, coupling the plastic lens and the rigid substrate. Several generations of ADG Fresnel lenses have been prototyped and experimentally characterized proving the achromatic behavior [18] as well as a strongly reduced temperature dependency [19]. Moreover, some prototype modules have been assembled and measured outdoors demonstrating that the achromatic performance of the ADG Fresnel lens has a reduced dependence with the CPV operating conditions such as ambient temperature and light spectrum [20].

The ADG concept, unlike previous achromatic theoretical studies, aimed at low cost manufacturability. Consequently, because of reasons strictly related to off-the-shelf materials available in the market, an architecture based on an encapsulant with low-index/low-dispersion was chosen. There are several low dispersion encapsulants developed for the PV industry which made it possible and affordable.

However, an inverted ADG architecture using a high-index/high-dispersion encapsulant has potentially higher efficiency. In this article, the authors present the results of a comprehensive analysis showing the potential improvement of the ADG technology achieved by switching from one architecture to the other. In section 2, the geometrical losses associated to both ADG architectures are compared, showing the potential of the inverted ADG lens. Section 3 focuses on the material requirements for the inverted ADG lens, reviewing the existing materials and providing the specifications for the required high-dispersion elastomer. Finally, section 4 addresses a comparative analysis of both architectures, showing that inverted ADG might achieve

a higher optical efficiency, which matches the conventional SoG efficiency while maintaining the advantages provided by the achromatic design demonstrated with the former design.

## 2. Optical losses in ADG Fresnel lenses

The losses associated to a Fresnel doublet can be divided into three groups: Fresnel reflection losses, absorption losses, and geometrical losses due to the Fresnel structure, this last caused in turn by draft angles, tips rounding, and rays lost at facets edge and lens perimeter.

On one side, reflection and absorption losses can be limited but not avoided and are strictly related to the optical properties of the materials used to manufacture the doublet. On the other side, the geometrical losses are mainly caused by switching from an aspheric profile to a Fresnel structure, which is essential in conventional CPV to reduce the volume, cost, and light absorption of the materials.

As already mentioned, the manufacturing process of the ADG Fresnel lens implies the lamination of the doublet over a rigid glass substrate. Therefore, only the architectures whose upper surface (the one facing the sun) is flat are suitable for this manufacturing approach.

An achromatic doublet must include a converging lens and a diverging lens manufactured in materials with different optical dispersion [13]. Additionally, the doublet must satisfy the achromaticity condition which is defined as:

$$f_1 V_1 + f_2 V_2 = 0 \quad (1)$$

where  $f_1$  and  $f_2$  are the focal distances of the individual lenses composing the doublet and  $V_1$  and  $V_2$  are the Abbe numbers of the materials used to manufacture them. The Abbe number is a measure of the material dispersion: the lower the Abbe number, the higher the dispersion [13,21]. Since the global focal distance of the doublet ( $f$ ) must be positive, the converging lens must be faster (*i.e.* shorter focal distance) than the diverging lens. Consequently, the Eq. (1) imposes that, in order to achieve an achromatic doublet, the positive lens must be manufactured using the material with low dispersion (high Abbe number) and the negative lens with the material with high dispersion (low Abbe number). Otherwise the design will increase the achromatic dispersion instead of compensating it. Consequently, only two architectures are possible:

1. low-refractive-index/low-dispersion positive lens facing the sun and high-refractive-index/high-dispersion negative lens toward the receiver;
2. high-refractive-index/high-dispersion negative lens facing the sun and low-refractive-index/low-dispersion positive lens toward the receiver.

The first corresponds to the classic ADG Fresnel lens [17–20] while the second is what we call the *inverted ADG*. Even if these two configurations perform very similar when they are designed to be aspheric, significant differences can be noticed when they include a Fresnel structure. Figure 1(a) and 1(b) show schematically the geometrical losses of the aspheric lenses caused by the opening of the beam in the first interface. Regardless of the chosen architecture, there are inevitably some rays lost in the perimeter of the lens. Nevertheless, this source of geometrical losses has a very limited impact on the optical efficiency.

Conversely, the geometrical losses are significantly different when both architectures are used in a Fresnel structure, shown in Fig. 1(c) and 1(d). The Fresnel facets are designed to work in pairs, so the light refracted at one facet of the first interface impinges at its corresponding facet pair in the second interface. The reader should note the shift between facet pairs, needed to compensate for the change of direction of the beam at the first interface. This shift must be optimized to minimize the light power that, instead of impinging on the corresponding facet, is transferred to an adjacent facet in the second interface, which would lead to a wider focused light spot and consequently to a reduced maximum concentration ratio.

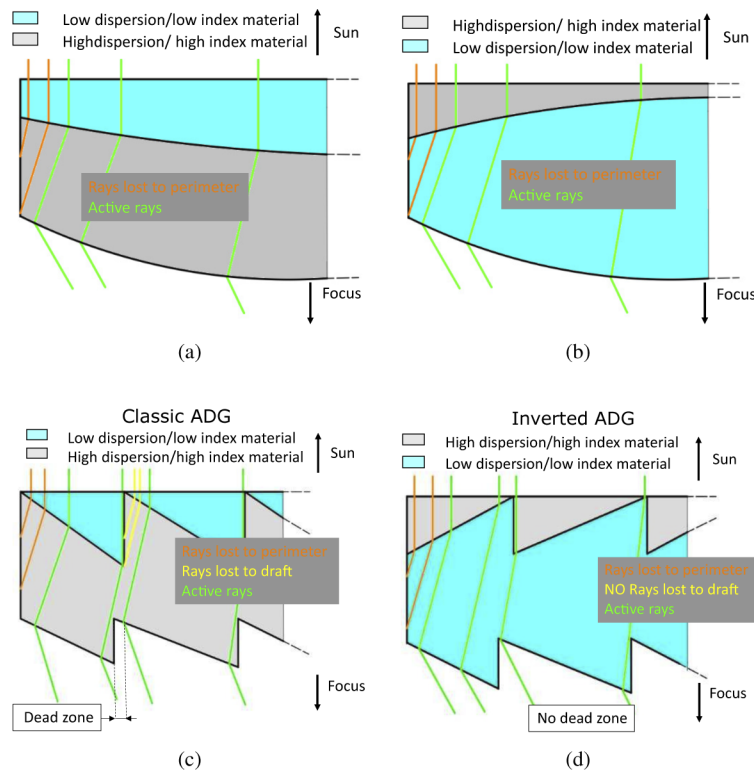


**Fig. 1.** Schematic representation of four possible configurations of an achromatic doublet. (a) Aspheric profile with the low-dispersion/low-index material on top of the high-dispersion/high-index material. (b) Aspheric profile with the high-dispersion/high-index material on top of the low-dispersion/low-index material. (c) Fresnel profile with the low-dispersion/low-index material on top of the high-dispersion/high-index material (classic ADG). (d) Fresnel profile with the high-dispersion/high-index material on top of the low dispersion/low index material (inverted ADG).

In the classic ADG (Fig. 1(c)), there are geometrical losses associated to the inherent discontinuities of a Fresnel lens because some rays refracted at the first interface do not reach its corresponding facet at the second interface, but get lost hitting the vertical wall of an adjacent facet in the first interface. This mechanism of loss does not take place with the inverted ADG architecture (Fig. 1(d)), which may result in a significantly higher attainable efficiency.

### 3. Materials

The choice of the pair of materials is essential to reach a cost-competitive ADG lens. As a matter of fact, the selected materials, apart from satisfying the achromaticity condition, Eq. (1), must be compatible for the lamination process, considering the ranges of temperature and pressure involved, and reliable for long term operation.

Nowadays, the PV market offers a wide range of materials which have been deeply and comprehensively studied [22–27]. Figure 2 shows the refractive index vs. the *solar Abbe number* of a selection of potential material investigated for the ADG concept. The Abbe number is a figure of merit used to determine a material dispersion in the visible range of the spectrum (the higher the Abbe number, the lower the dispersion) [13]. The solar Abbe number is an equivalent figure of merit defined to measure the material dispersion in a wider spectral range, specifically in

the spectral range of interest of a conventional MJ solar cell (350 – 1700 nm). For its calculation, 400 nm has been selected as *blue* wavelength and 1000 nm as *red* wavelength, considering that refractive index is fairly constant between 1000 nm and 1700 nm. The development of the classic ADG lens was based on a thermoplastic elastomer (TPE) as low dispersion material and polycarbonate (PC) as high dispersion material. This pair of materials fulfilled the requirements stated above: compatibility and potentially low cost of both materials and manufacturing process. The selected TPE can be processed at low temperatures compatible with the PC, so the laminating process took place at temperatures around 120 °C [28]. Being the elastomer the low-index/low-dispersion material, it necessary constitutes the material of the converging lens, resulting in the architecture characterized by more dead zones caused by the vertical walls of the Fresnel facets (Fig. 1(c)). As discussed in the previous section, such architecture results in a limited maximum efficiency. Furthermore, in order to avoid the yellowing of the PC due to exposition to ultra-violet (UV) radiation [29–31], blocking UV radiation is required, with an obvious detrimental impact on the transmitted radiant flux.

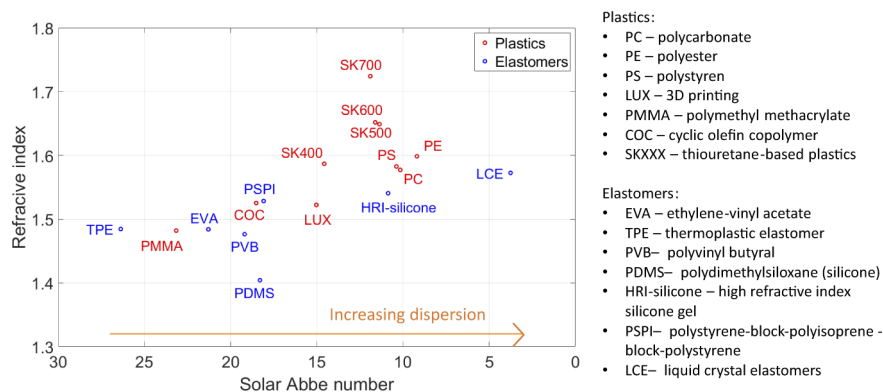


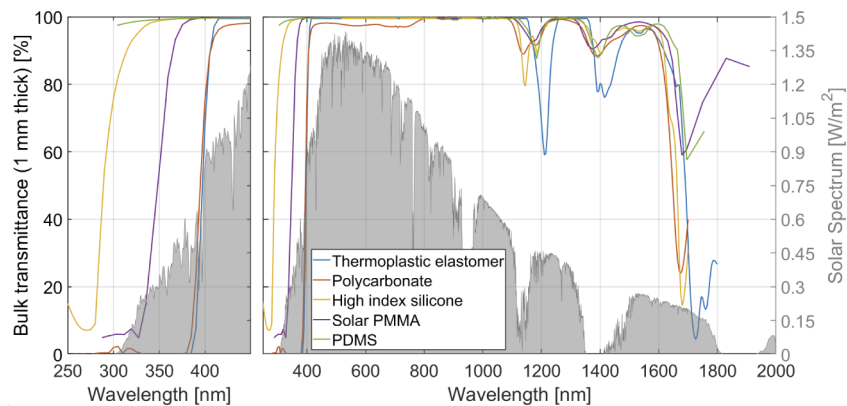
**Fig. 2.** Dispersion graph representing the refractive index and the solar Abbe number for all the plastics and the elastomers investigated.

The inverted ADG Fresnel lens (high dispersion/high index material on top of the low dispersion/low index material) requires the identification of a pair of materials suitable for this architecture: a high-index/high-dispersion encapsulant and a low dispersion/low index moldable material.

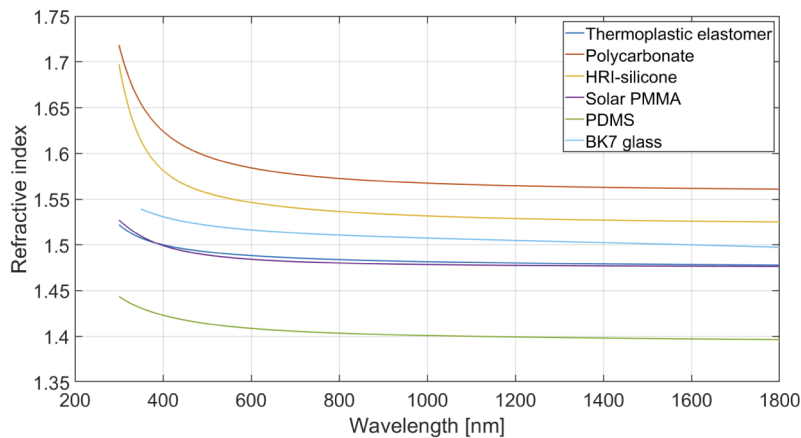
For the encapsulant, high dispersion materials are not as available in the market as low dispersion ones. There are also additional requirements for the encapsulant, namely UV resistance, good adhesion to glass and to the low-dispersion material, and low cost. For the case of study of this paper, we have selected a high refractive index (HRI) silicone developed for high intensity LED applications which fulfills the optical requirements and the demanded material compatibility. It is a clear, soft silicone gel that cures at room temperature, it is UV resistant, and provides good adhesion (with or without the use of prime, depending on the formulation). For what concern the low-index/low-dispersion material the best option is PMMA. It is cheap, easily moldable by injection and compression molding processes, withstands solar radiation, and has a proved long-term reliability in CPV applications [32]. Noteworthy, there are PMMA specific formulations for solar applications that withstand UV radiation. Since CPV industry has extensive experience in the use of silicones for manufacturing SoG Fresnel lenses [5-6], the manufacturing process of the inverted ADG may be similar to the SoG process, with the only difference that the rubber or metallic mold used for the shaping of the SoG parquet is no longer needed because the plastic lenses themselves act as the mold.

However, a conventional optical-grade PDMS is proposed as a possible alternative for the low-dispersion/low-index material. Both the transmission properties and the dispersion of PDMS are similar to PMMA's, making the pair HRI-silicone/PDMS optically compatible with the inverted ADG architecture. Such design, being composed of two encapsulants, requires a different manufacturing process. The inverted ADG lens might be obtained by *double lamination*, *i.e.* laminating the first HRI-silicone layer as it was a conventional SoG lens and then laminating the PDMS layer on the top in a second step.

Figure 3 shows the transmittance and the refractive index as functions of light wavelength for the materials used in the classic ADG and the materials proposed for the inverted ADGs. As it will be disclosed in section 4, the maximum thickness of the studied achromatic lenses is 1 mm. Therefore, for the transmittance, a sample's thickness equal to 1 mm has been chosen for every material to consider a worst-case scenario. First, observing Fig. 3(a), the combined transmission of TPE and PC is lower than the combined transmission of HRI-silicone and PMMA or HRI-silicone and PDMS, due to the high TPE absorption in the UV region. For the PC, although a formulation that does not block entirely the UV radiation was chosen, it shows lower



(a)



(b)

**Fig. 3.** (a) Spectral transmittance of the materials used for both the classic ADG (TPE and PC) and the new ADG (HRI-silicone, PMMA, and PDMS). (b) Refractive index of the materials used for both the classic ADG (TPE and PC) and the new ADG (HRI-silicone, PMMA, and PDMS). The refractive index of BK7 glass is also shown as reference.

performance in the UV-visible region compared with the other materials. Conversely, the solar PMMA formulation, that is a specific composition designed for solar energy applications, does not block UV radiation and does not require UV blocking to avoid yellowing. Second, because of the high PC refractive index, in the classic ADG design losses due to Fresnel reflection when light crosses the PC-air interface are higher than crossing either PMMA-air or PDMS-air interfaces. Furthermore, Fresnel reflections taking place within the ADG lens, despite they are very low, are also reduced in the inverted architectures. As it is shown in Fig. 3(b), the refractive index of BK7 glass, HRI-silicone, and PMMA are very close, while PC has a higher index than TPE.

#### 4. Comparative analysis of different architectures

A comprehensive set of Monte Carlo ray-tracing simulations was carried out with a commercial software in order to assess the advantages provided by the inverted ADG configuration with respect to the classic architecture. The two main figures of merit investigated are the optical efficiency and the maximum attainable concentration, which are the two parameters that best characterize a concentrator optics. Moreover, these two figures of merit will be analyzed simulating the system at different operating temperatures.

The Fresnel lenses simulated are the classic ADG, composed of a TPE as elastomer and PC as rigid material, the inverted ADG, composed of HRI-silicone and PMMA, and the inverted ADG manufactured in silicones - the conventional PDMS and the high index HRI-silicone. A conventional SoG Fresnel lens is also simulated as a benchmark.

The following list summarizes the lens parameters and the assumptions made for the ray-tracing simulations. All are exactly the same for all the lens types, except the lens thickness, which also determines the number and dimensions of the facets. As explained in Fig. 1, geometrical losses differ depending on lens type. Generally, the optimum thickness balances absorption and geometrical losses, considering that the thicker the lens the higher the absorption losses and the lower the number of Fresnel facets (*i.e.*, the lower the losses related with tips rounding of peaks and valleys). For a fair comparison, the lens thickness has been optimized for each case:

- thickness of simulated lenses:
  - the minimum height of the lens facets can be only a few tens of microns for the case of SoG. In addition, a thin silicone layer is also required to assure a good adhesion to the glass. Considering both, the optimum lens thickness is 0.6 mm for the SoG design. This value is dependent on the rest of the parameters listed below, for instance a reduction of the tips rounding would lead to a lower thickness;
  - the minimum manufacturable lens thickness, for the case of the ADG lenses, is 1 mm, considering that it involves the molding of a plastic piece. For both classic and inverted ADGs, this minimum thickness provides also the optimum performance. Nevertheless, it must be pointed out that the classic ADG requires a hot lamination, while the inverted ADG described in this paper can be manufactured with a room temperature lamination. In our experience, a higher thickness, typically around 2 mm, is required to keep the optical quality of the plastic piece after the hot lamination;

based on this considerations, to present a fair comparison between the classic and the inverted ADG architectures, the same thickness equal to 1 mm has been chosen. However, let consider that for the classic ADG increasing the lens thickness up to 2 mm results in additional efficiency loss equal to 1.6%.

- all the simulated lenses are square of 40x40 mm<sup>2</sup>, designed with curved facets;
- tips rounding are estimated equal to 3 μm. Same value assumed for all lenses;

- draft angles are increasing from  $2^\circ$  to  $5^\circ$  going from the center to the corners of the lens. Same value assumed for all lenses;
- the real sun angular size ( $\pm 0.27^\circ$ ) and the reference spectrum AM1.5D (IEC 60904-3) for direct normal irradiance (DNI) are assumed;
- the receiver is considered to be ideal, *i.e.*, absorbing all the impinging irradiance for the whole spectral range;
- spectrally resolved transmittance and refractive index are used for all materials involved in the simulations;
- the surfaces are considered ideal (no roughness, waviness or shape errors) and the optical system perfectly aligned with the light source.

#### 4.1. Optical efficiency

Figure 4 shows the optical efficiencies of the four lenses included in the set of ray-tracing simulations carried out. First, the simple bars show the *transmission efficiency* with a reference solar spectrum AM1.5D divided by spectral ranges roughly coincident with the subcells of a conventional triple junction (3J) solar cell. Second, the bars with the dashed pattern represent the lens efficiency weighted with the spectral response (SR) of the top, middle, and bottom subcells of a commercial triple-junction (3J) solar cell upright metamorphic (GaInP/GaAs/Ge 1.82/1.33/0.67 eV).

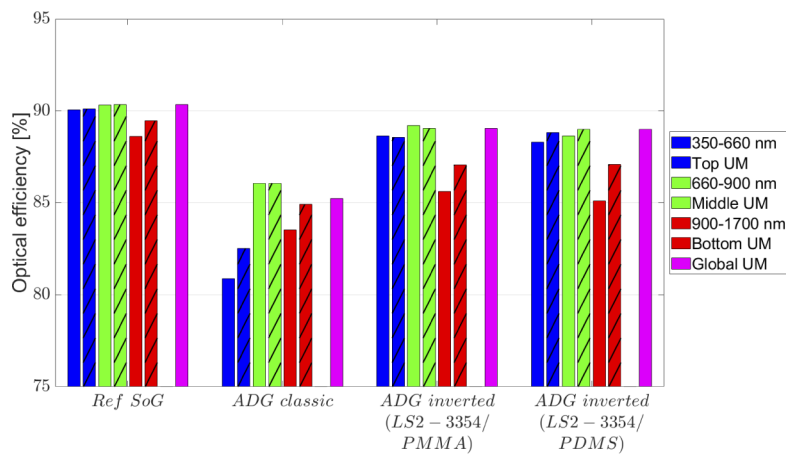


**Fig. 4.** Optical efficiency simulated for the four lenses included in the analysis. The filled bars represent the pure transmission efficiency in three different spectral ranges. The bars with the dashed patterns represent the efficiencies when the transmitted radiant power is weighted with the subcells SR of a 3J upright metamorphic solar cell.

For the latter, the light source is divided in three sub-sources: one for each subcell. Each of the three sources has the direct normal AM1.5 spectral irradiance distribution as described in IEC 60904-3, but normalized to  $1000 \text{ W/m}^2$ , and is then multiplied with the SR of the respective subcell. Spectral responses instead of quantum efficiencies are preferred in the simulation because the final goal is to determine the current generated by each subcell. The magenta column is the *global efficiency* which is defined as the ratio between the current generated by the 3J solar cell (minimum value among top, middle, and bottom subcells) and the current generated by a bare 3J solar cell of the same technology whose size is equal to the lens aperture. To conclude, in all

simulations the receiver size has been chosen large enough to ensure that all the light transmitted by the lens is captured by the receiver. Hence, the optical efficiency presented does not take into account the concentration capability of the optics.

First, thanks to its reduced thickness (0.6 mm against 1 mm for both the classic and the inverted ADGs) and to the high transparency of the PDMS, the reference SoG has the highest efficiency in all ranges. The absorption peaks in the NIR region cause the slightly lower bottom efficiency. Second, due to the high number of dead zones, the ADG classic has the lowest efficiency in all ranges. Furthermore, the top efficiency is even lower because of the UV blocking TPE used as encapsulant required to protect the PC from yellowing. Finally, both the inverted ADGs show significant improvement compared to the classic ADG even though they do not achieve the efficiency value of a conventional SoG. Moreover, it is worth to notice that both inverted ADGs have much lower bottom efficiency than top and middle. As well as for the reference SoG, this is caused by the absorption peaks of the PMMA and PDMS in the NIR region, which are more significant because of the thicker substrate. However, the decrease of the transmitted radiant power corresponding with the bottom range (900 – 1700 nm) are generally negligible for 3J solar cell based on a bottom subcell of Germanium (0.67 eV), which usually generates a significant excess of current, so a higher absorption (*i.e.* lower efficiency) in that range does not affect the global efficiency of the CPV system, as it is demonstrated observing the global efficiency bar which is almost equal to top and middle efficiencies.

#### 4.2. Attainable concentration

Figure 5(a) shows the optical efficiency of each lens as a function of the solar cell radius in the whole spectral range of interest (350 – 1700 nm). This figure of merit is obtained by processing the irradiance meshes cast by the lenses and shown in Fig. 5(b). The percentage of the transmitted power contained within several circles having different radius is multiplied by the optical efficiency of each simulated lens. It can be noticed that all ADGs exhibit a significantly higher concentration capability than the conventional SoG. If we define the maximum attainable concentration as corresponding with the smallest receiver capable of capturing the 99% of the transmitted power, the SoG is limited to a maximum value of 400 *suns*, while the ADGs achieve values around 1200 *suns* (1200 *suns* for the inverted ADG HRI-silicone/PMMA and 1150 *suns* for both the ADG inverted HRI-silicone/PDMS and the classic ADG classic).

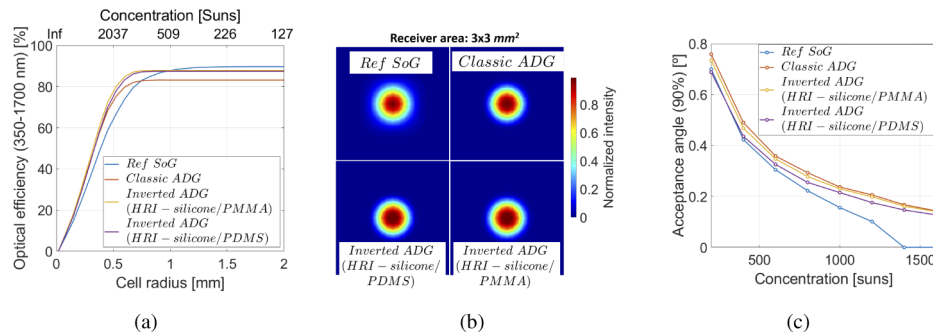


**Fig. 5.** (a) Optical efficiency as a function of the receiver radius (*i.e.* the concentration) for both the classic and inverted ADG Fresnel lenses. The efficiency of a conventional SoG Fresnel lens is also shown as reference. (b) Irradiance meshes of the four simulated Fresnel lenses. (c) Acceptance angle (90% of efficiency) of the lenses as a function of the geometrical concentration.

However, it can be observed that, despite the maximum attainable concentration of the reference SoG lens was 400 *suns*, the optical efficiency of the SoG remains higher up to a concentration

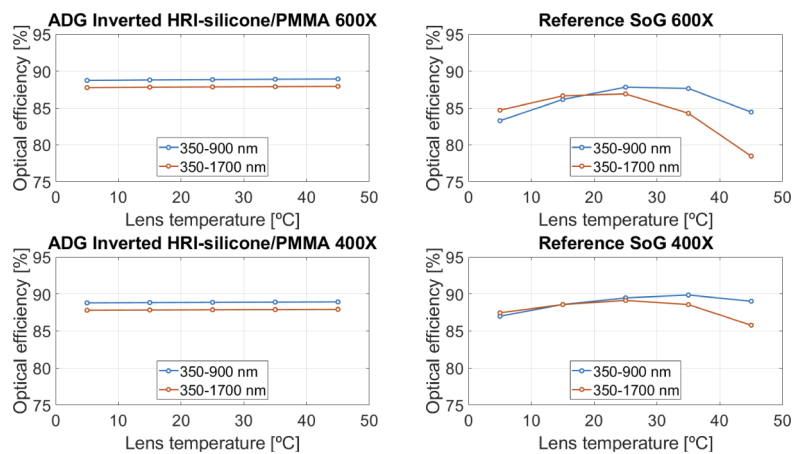
value equal to 530 *suns* (inverted ADG with PMMA) and to 560 *suns* (inverted ADG with PDMS).

Figure 5(c) shows the acceptance angle of the system as a function of the geometrical concentration. The acceptance angle is defined as the misalignment angle required to drop the efficiency below the 90% of its maximum (where the maximum is defined as the transmission efficiency at low concentration) while the geometrical concentration is the ratio between the lens aperture and the receiver area. Despite the maximum attainable concentration of both inverted ADGs is three times the maximum attainable concentration of the reference SoG, Fig. 5(c) shows only a marginal benefit in terms of acceptance angle for a given geometrical concentration factor. For instance, considering a geometrical concentration of about 400 *suns* (reasonable choice in a commercial CPV system based on SoG without any SOE), switching from conventional SoG to the ADG design the acceptance angle only increases from  $0.42^\circ$  to  $0.49^\circ$ . This is due to the physical limitation proper of every concentrating system. As a sake of example, based on simple geometrical consideration, a concentrating lens with f-number equal to 1.4 and a concentration factor of 400 *suns*, even considering a perfectly collimated light source and no chromatic aberration, would have an acceptance angle of  $0.7^\circ$ . Consequently, the attenuation of the color dispersion provided by the achromatic design does actively push the acceptance angle toward its physical limit, but only in a reduced extent.

However, the highest concentration capability is only one of the advantages provided by the proposed achromatic design. In fact, as it will be disclosed in the next section, the achromatic behavior of the lens together with the reduced spot size and the lower temperature sensitivity of the chosen materials provide a highly enhanced stability against temperature changes.

#### 4.3. Temperature dependency

Silicone on glass lenses have a very strong temperature dependence [33–35] mainly caused by the variation of the refractive index of the optical materials but also by the slight deformation of the facets caused by the thermal stress. During the manufacturing process, SoG lenses can be optimized for best performance at a given temperature, typically 35 – 40°C, which corresponds to 10 – 15°C above an ambient temperature of 25°C [36].



**Fig. 6.** Optical efficiency as a function of the operating temperature of the lens simulated at two different concentration factors: 400 *suns*, and 600 *suns*.

In order to demonstrate the reduced temperature dependency of the ADG design, several simulations have been carried out varying the refractive index of the material involved following the Claussis-Mossoti equation [11]. In Fig. 6, the optical efficiencies of the inverted ADG (version

with PMMA) and the reference SoG are shown as a function of the lens temperature which has been varied between 5 °C and 45 °C. It is worth to notice that the simulation only take into account the refractive index variation. The deformation of the lens profile is not included. Finally, the inverted ADG with PDMS is not included because equivalent results have been obtained. The simulation have been carried out considering two scenarios: firstly, the scenario corresponding to the maximum attainable concentration for the reference SoG (400 *suns*). Secondly, a high concentration scenario were the advantage of the new technology results to be more relevant.

For the 400 *suns* scenario it can be noticed that when the temperature is either high or low the higher temperature sensibility of the reference SoG causes its efficiency to drop below the ADG's, whose value remains constant along all the temperature range. As a consequence, the overall performance of a CPV system based on SoG lenses has a significant yearly variation under sun exposure [34]. Moreover, in the high concentration scenario the reference SoG is not capable of concentrating all the light over the solar cell surface, exhibiting a lower efficiency also when the temperature is the optimal. Furthermore, also a slight temperature variation supposes an efficiency decrease. Conversely, the inverted ADG also in this scenario exhibits a constant efficiency in the whole temperature range.

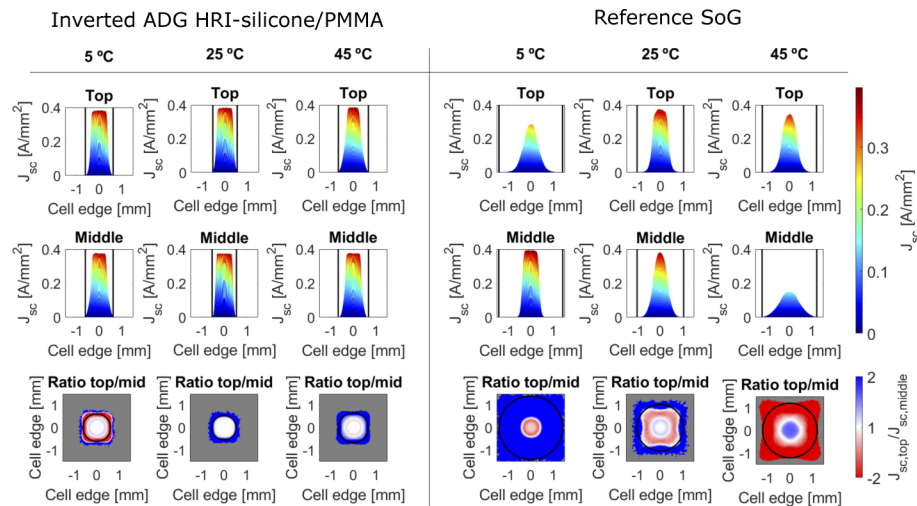


**Fig. 7.** Spatial distribution of the photogenerated current for the top  $J_{sc}^{top}$  (first row) and middle  $J_{sc}^{mid}$  (second row) subcells at different temperatures predicted by ray-tracing simulations. Contour graphs (third row) show the ratio between top and middle photocurrents  $J_{sc}^{top} / J_{sc}^{mid}$ . In the contour graphs, blue areas represent cell regions where there is an excess of top photogenerated current (middle-limited device) while red areas represent an excess of middle photogenerated current (top-limited device). Regions where both subcell photocurrents are matched are shown in white. Gray areas represent regions where both photocurrent values are below 0.1% of the maximum, that is, dark areas. The black circles in the third row and the black vertical lines in the first two rows represent the spot size calculated as the circle containing the 99% of the energy collected by the receiver.

Moreover, the achromatic design intrinsically provides a more uniform light distribution over the solar cell surface. Non-uniformities, where the spectral content of the flux varies across the cell, are inherent to refractive CPV systems because of the optical transfer function and chromatic aberration in the optics. When the photogenerated current distribution are such that there are different regions over the cell either limited by the top or the middle subcell, the limiting subcell will be determined by the resistance of the layers connecting the subcells [37–40]. The result of this uneven spatial distribution for each subcell may cause additional current loss at spectral

conditions where the subcells are current matched, this effect is well explained in [38]. Figure 7 shows the photogenerated current for the top and middle subcells. The current density of each subcell is obtained weighting the transmitted power with the subcell's SR, as well as has been done in section 4.1 to get subcells' efficiencies. As it can be observed in Fig. 7, the ADG Fresnel lens does not only cast a smaller irradiance spot but it provides two additional benefits compared to a classic SoG Fresnel lens. In the first place, the photogenerated current distributions for top and middle subcells are much more similar reducing the losses associated with lateral current flows. In the second place, the irradiance distribution is less sensitive to the temperature of the primary lens. This thermal sensitivity is one of the main drawbacks of SoG Fresnel lens [33,41,42] and reducing its impact on the irradiance distribution over the cell is expected to increase the energy harvested throughout the year [34]. To conclude, it is worth to notice that the PMMA used for manufacturing the inverted ADG has a much lower coefficient of thermal expansion (CTE) in comparison with PDMS. This suggests that, if deformation were included in the simulation model, they would affect in a higher extent the reference SoG technology with respect to the ADG, further increasing the advantage of the latter with respect to the former.

#### 4.4. Breakdown of optical losses

Earlier in section 2, the main sources of losses have been listed. In Fig. 8 such losses are represented in a Sankey diagram for the reference SoG Fresnel lens and for both the classic and inverted ADG designs. Only the HRI-silicone/PMMA ADG inverted is shown because the source of losses of the HRI-silicone/PDMS is similar and no additional information can be drawn.

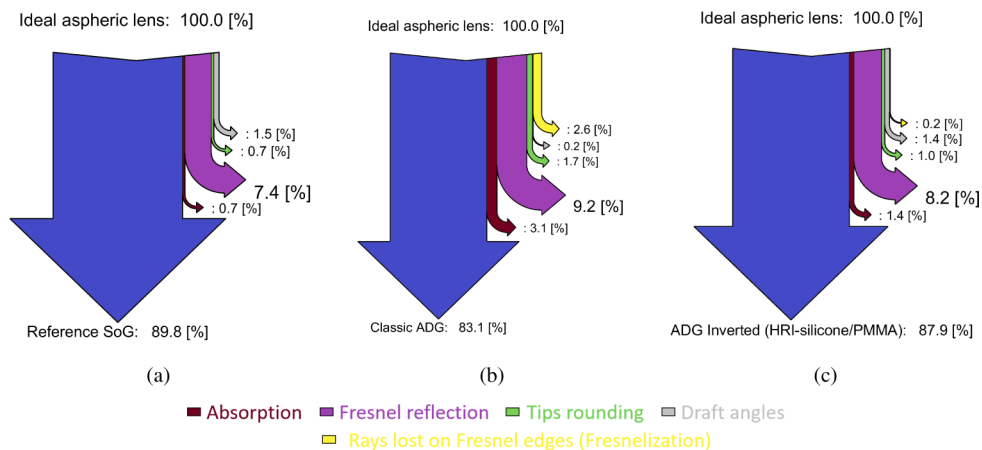


**Fig. 8.** Sankey diagram showing the losses of (a) the reference SoG Fresnel lens, (b) the classic ADG Fresnel lens design, and (c) the inverted ADG Fresnel lens design (HRI-silicone/PMMA). The diagram is not in scale.

The reference SoG, as expected, shows the lowest losses. The low refractive index of PDMS (ca. 1.4) results in lower Fresnel reflection in the air-PDMS interface and the thinner design in very low absorption. Conversely, the classic ADG, being thicker than the SoG, shows very high absorption, further increased by UV blocking of the TPE. However, the inverted ADG architecture, thanks to the improved transmittance of the chosen material, only loses 1.4% of efficiency in absorption. Despite this number is still the double than the reference SoG, a significant improvement has been achieved in comparison with the former ADG design.

Concerning the Fresnel reflection, the inverted design implies an improvement with respect to the classic design. This is due to the lower refractive index of both PMMA and HRI-silicone (ca. 1.5) with respect to the PC (ca. 1.6). The last significant difference between the two ADG

designs is the geometrical loss related to the *Fresnelization* (yellow in Fig. 8) of the lens, that is switching from an aspherical profile to a profile including Fresnel facets. As explained in section 2, the classic ADG loses 2.6% of the transmitted radiant power at the vertical walls of the Fresnel facets. Conversely, the losses in inverted ADG design are negligible (estimated to be approximately 0.2%). As mentioned in section 4, it is worth to notice that the simulated classic ADG have been chosen to be as thick as the inverted ADG. However, if a thickness of 2 mm would be used to ensure its resistance to the hot lamination process, the optical efficiency would reduce of additional 1.6% because of increased absorption and slightly increased Fresnelization, widening further the difference between classic and inverted architecture.

The Sankey diagrams shown in Fig. 8 are obtained simulating the losses along all the spectrum of interest for a 3J solar cell (350 – 1700 nm). As observed in section 4.1, losses caused by the absorption peaks in the NIR region are negligible when a 3J solar cell based on Germanium is used. Therefore, considering only the spectral ranges of top and middle subcells (350 – 900 nm) the absorption losses of the inverted ADG drops down to 0.4%, for an optical efficiency of 88.9%.

In order to minimize the transmission losses of a concentrating Fresnel lens, it is important to identify which lens parameters are responsible for every specific loss. For instance, the geometrical losses (draft angles, tips rounding, and Fresnelization) are caused by the Fresnel facets. Conversely, the bulk absorption is related to the thickness of the materials that light must go through. The optimum design must be a tradeoff between these two losses: the lower number of facets (thicker lens) the lower geometrical losses and the higher absorption losses. Note that the number of facets affects only the tips rounding losses. For the same design, the draft angle losses are equal regardless the number of grooves and cannot be reduced without reducing the draft angle value (manufacturing issue). The reference SoG design used as benchmark is the FLATCON™ module [43], which is a widely known CPV system based on SoG Fresnel lenses and whose design has been exhaustively optimized both theoretically and using data from operation [44]. The inverted ADG analyzed in this work have been optimized to be as thin as possible without drastically increase geometrical losses, resulting in very low absorption if compared with the classic design. However, other parameters such as the f-number have been chosen similar to the benchmark technology, without a dedicated optimization.

To conclude, the ADG inverted architecture overcame the main limitations of the classic design, namely the geometrical losses due to the dead zones of the lens profile and the high absorption in the UV region. However, further improvement is still possible, especially if the specific application and the CPV system type where the ADG would be used were inputs in the optimization process.

## 5. Conclusion

In this work a novel ADG Fresnel lens design has been presented and analyzed. Two different pairs of material have been studied: the first is composed of a high refractive index silicone and a solar PMMA, while the second is composed of the same HRI-silicone and a conventional PDMS. Both designs show similar performance.

The proposed architecture, provides several advantages compared to previous designs based on lamination of a polycarbonate (PC) bi-Fresnel sheet on a glass by means of a low dispersion thermoplastic elastomer (TPE). Firstly, it avoids the intrinsic geometrical losses caused by the rays that, in the former ADG design, hit the vertical wall of the Fresnel facets (dead zones). Such improvement alone results in an efficiency increase equal to 2.6%. Secondly, the combined absorption of the HRI-silicone and PMMA (or PDMS) is lower than the combined absorption of the TPE and PC used in the classic ADG. The classic ADG requires UV blocking in order to avoid the yellowing of the PC, limiting the transmission efficiency in the top subcell region. Conversely, the solar PMMA used in the inverted ADG, as well as the PDMS, does not filter the UV light and does not get yellow, ensuring improved transmission and longer durability. This

improvement resulted in an efficiency increase equal to 1.6%. Therefore, the global transmission efficiency of the inverted design is equal to 87.9%, much higher than the classic design (83.1%) and very close to the reference SoG used as benchmark (89.8%). Moreover, if a 2 mm thick classic ADG Fresnel lens would have been considered, the increased absorption would result in additional 1.6% of losses further enhancing the benefit of the inverted design.

Despite the achieved efficiency is still 2% lower than the reference technology, the achromatic behavior of the inverted ADG Fresnel lens provides several advantages. On the one hand, the concentration capability of both the inverted designs is approximately equal to the classic ADG (maximum concentration of 1150 *suns*), and much higher than a conventional SoG Fresnel lens (maximum 400 *suns*). The inverted ADG manufactured in PMMA may achieve a concentration of 1200 *suns* without any light spillage, which is three times a conventional SoG lens. The inverted ADG including PDMS achieves 1150 *suns*, which is still much higher than the SoG. The higher attainable concentration provides several advantages: firstly it is possible to slightly improve the concentration-acceptance angle product (CAP) which can provide either higher concentration maintaining system tolerances or the same concentration improving system tolerances. Secondly, the smaller spot size significantly reduce the temperature dependency of the lens. The simulations carried out showed that, also in a high concentration scenario (600 *suns*), the optical efficiency of the ADG lens remains equal to its maximum in the whole simulated temperature range (5 °C - 45 °C). On the other hand, the achromatic behavior of the ADG lenses results in a much more uniform light distribution over the solar cell surface in the whole simulated temperature range, reducing the losses associated with lateral current flows and potentially enhancing the yearly energy harvesting.

To summarize, the new ADG Fresnel lens design provides higher optical efficiency and similar maximum attainable concentration maintaining, at the same time, all the advantages of the achromatic design previously demonstrated for the classic ADG architecture (reduced thermal sensitivity, more uniform light distribution over the receiver, and slightly higher CAP). Furthermore, the manufacturing process envisaged for the ADG inverted is simple, cost-effective, and scalable.

Finally, it is worth to remark that this technology may achieve even better performances if applied in the Micro-CPV field (solar cell diameter less than 1 mm), where the reduced dimensions involved allow to reduce the number of grooves without increasing the thickness of the lens, with the potential of manufacturing a lens where the only significant losses consist in the Fresnel reflection.

**Funding.** Horizon 2020 Framework Programme CPVMatch project (640873); Ministerio de Economía, Industria y Competitividad, Gobierno de España Micro-PV project (ENE2017-87825-C2-1-R).

**Acknowledgments.** A special thanks to David Miller from the National Renewable Energy Laboratory (NREL) for providing materials transmittance data used in this work.

**Disclosures.** The authors declare no conflicts of interest.

**Data availability.** Data underlying the results presented in this paper are not publicly available at this time but may be obtained from the authors upon reasonable request.

## References

1. M. Steiner, G. Siefer, T. Schmidt, M. Wiesenfarth, F. Dimroth, and A. W. Bett, "43 % direct sunlight conversion efficiency using 4J cells with achromatic full glass lens," in *CPV-12*, (Freiburg, Germany, 2016), p. 080006.
2. M. Steiner, M. Wiesenfarth, J. F. Martínez, G. Siefer, and F. Dimroth, "Pushing energy yield with concentrating photovoltaics," in *15th International Conference on Concentrator Photovoltaic Systems (CPV-15)*, (Fes, Morocco, 2019), p. 060006.
3. M. A. Green, E. D. Dunlop, D. H. Levi, J. Hohl-Ebinger, M. Yoshita, and A. W. Ho-Baillie, "Solar cell efficiency tables (version 54)," *Prog. Photovoltaics* **27**, 565–575 (2019).
4. J. F. Geisz, R. M. France, K. L. Schulte, M. A. Steiner, A. G. Norman, H. L. Guthrey, M. R. Young, T. Song, and T. Moriarty, "Six-junction III–V solar cells with 47.1% conversion efficiency under 143 Suns concentration," *Nat. Energy* **5**(4), 326–335 (2020).

5. C. Algora and I. Rey-Stolle, eds., *Handbook of Concentrator Photovoltaic Technology* (Wiley, Chichester, West Sussex, United Kingdom, 2016).
6. M. Wiesenfarth, I. Anton, and A. W. Bett, "Challenges in the design of concentrator photovoltaic (CPV) modules to achieve highest efficiencies," *Appl. Phys. Rev.* **5**(4), 041601 (2018).
7. E. Lorenzo and G. Sala, "Hybrid silicone-glass Fresnel lens as concentrator for photovoltaic applications," in *Sun II*, (1979), pp. 536–539.
8. I. Antón, D. Pachón, and G. Sala, "Characterization of optical collectors for concentration photovoltaic applications," *Prog. Photovoltaics* **11**, 387–405 (2003).
9. M. Victoria, S. Askins, R. Herrero, I. Antón, and G. Sala, "Assessment of the optical efficiency of a primary lens to be used in a CPV system," *Sol. Energy* **134**, 406–415 (2016).
10. G. Vallerotto, M. Victoria, S. Askins, I. Antón, G. Sala, R. Herrero, and C. Domínguez, "Indoor Experimental Assessment of the Efficiency and Irradiance Spot of the Achromatic Doublet on Glass (ADG) Fresnel Lens for Concentrating Photovoltaics," *J. Visualized Exp.* **128**, 56269 (2017).
11. M. Victoria, "New concepts and techniques for the development of high-efficiency concentrating photovoltaic modules," Ph.D. thesis, E.T.S.I. Telecomunicación (UPM) (2014).
12. M. Victoria, C. Domínguez, I. Antón, and G. Sala, "Comparative analysis of different secondary optical elements for aspheric primary lenses," *Opt. Express* **17**(8), 6487–6492 (2009).
13. E. Hecht, *Optics* (Addison Wesley Longman, Inc., 1998), third edition ed.
14. F. Languy, K. Fleury, C. Lenaerts, J. Loicq, D. Regaert, T. Thibert, and S. Habraken, "Flat Fresnel doublets made of PMMA and PC: Combining low cost production and very high concentration ratio for CPV," *Opt. Express* **19**(S3), A280–A294 (2011).
15. F. Languy and S. Habraken, "Performance comparison of four kinds of flat nonimaging Fresnel lenses made of polycarbonates and polymethyl methacrylate for concentrated photovoltaics," *Opt. Lett.* **36**(14), 2743 (2011).
16. F. Languy, C. Lenaerts, J. Loicq, T. Thibert, and S. Habraken, "Performance of solar concentrator made of an achromatic Fresnel doublet measured with a continuous solar simulator and comparison with a singlet," *Sol. Energy Mater. Sol. Cells* **109**, 70–76 (2013).
17. G. Vallerotto, M. Victoria, S. Askins, R. Herrero, C. Domínguez, I. Antón, and G. Sala, "Design and modeling of a cost-effective achromatic Fresnel lens for concentrating photovoltaics," *Opt. Express* **24**(18), A1245–A1256 (2016).
18. G. Vallerotto, S. Askins, M. Victoria, I. Antón, and G. Sala, "A novel achromatic Fresnel lens for high concentrating photovoltaic systems," in *AIP Conference Proceedings*, vol. 1766 (AIP Publishing, 2016), p. 050007.
19. G. Vallerotto, M. Victoria, S. Askins, I. Antón, and G. Sala, "Experimental characterization of achromatic doublet on glass (ADG) Fresnel lenses," *AIP Conf. Proc.* **1881**, 030010 (2017).
20. G. Vallerotto, M. Wiesenfarth, M. Victoria, M. Steiner, I. Antón, N. Jost, S. Askins, and G. Sala, "Outdoor experimental characterization of novel high-efficiency high-concentrator photovoltaic (HCPV) modules using achromatic doublet on glass (ADG) Fresnel lenses as primary optics," *AIP Conference Proceedings* p. 030006 (2019).
21. H. Hovestadt, J. Everett, and A. Everett, *Jena Glass: And Its Scientific and Industrial Applications* (Macmillan, 1902).
22. R. H. French, J. M. Rodriguez-Parada, M. K. Yang, R. A. Derryberry, M. F. Lemon, M. J. Brown, C. R. Haeger, S. L. Samuels, E. C. Romano, and R. E. Richardson, "Optical properties of materials for concentrator photovoltaic systems," in *Photovoltaic Specialists Conference (PVSC), 2009 34th IEEE*, (IEEE, 2009), pp. 000394–000399.
23. D. C. Miller, M. D. Kempe, C. E. Kennedy, and S. R. Kurtz, "Analysis of transmitted optical spectrum enabling accelerated testing of CPV designs," in *High and Low Concentrator Systems for Solar Electric Applications IV*, vol. 7407 (International Society for Optics and Photonics, 2009), p. 74070G.
24. M. Kempe, "Overview of scientific issues involved in selection of polymers for PV applications," in *Photovoltaic Specialists Conference (PVSC), 2011 37th IEEE*, (IEEE, 2011), pp. 000085–000090.
25. B. Ketola and K. R. McIntosh, "Silicones for Photovoltaic Encapsulation," in *23rd European Photovoltaic Solar Energy Conference*, (2008).
26. K. R. McIntosh, J. N. Cotsell, J. S. Cumpston, A. W. Norris, N. E. Powell, and B. M. Ketola, "An optical comparison of silicone and EVA encapsulants for conventional silicon PV modules: A ray-tracing study," in *Photovoltaic Specialists Conference (PVSC), 2009 34th IEEE*, (IEEE, 2009), pp. 544–549.
27. T. Swonke and U. Hoyer, "Diffusion of Moisture and Impact of UV Irradiance in Photovoltaic Encapsulants," *24th European Photovoltaic Solar Energy Conference 21-25 September 2009*, Germany; 3373–3376 (2009).
28. G. Vallerotto, "Achromatic Doublet on Glass Fresnel Lenses for Concentrator Photovoltaic Systems," Ph.D. thesis, E.T.S.I. Telecomunicación (UPM) (2019).
29. F. Pern, A. Czanderna, K. Emery, and R. Dhere, "Weathering degradation of EVA encapsulant and the effect of its yellowing on solar cell efficiency," in *The Conference Record of the Twenty-Second IEEE Photovoltaic Specialists Conference - 1991*, (IEEE, Las Vegas, NV, USA, 1991), pp. 557–561.
30. A. L. Rosenthal and C. G. Lane, "Field test results for the 6 MW Carrizo solar photovoltaic power plant," *Sol. Cells* **30**(1-4), 563–571 (1991).
31. F. Pern and A. Czanderna, "Characterization of ethylene vinyl acetate (EVA) encapsulant: Effects of thermal processing and weathering degradation on its discoloration," *Sol. Energy Mater. Sol. Cells* **25**(1-2), 3–23 (1992).

32. B. Fassbender, P. Battenhausen, U. Löffler, J. Ackermann, P. Colburn, and P. A. Marks, "Reliability of PMMA for CPV Lens Applications," in *Proceedings of the ISES Solar World Congress 2011*, (International Solar Energy Society, Kassel, Germany, 2011), pp. 1–11.
33. S. Askins, M. Victoria, R. Herrero, C. Domínguez, I. Antón, and G. Sala, "Effects of Temperature on Hybrid Lens Performance," *AIP Conf. Proc.* **1407**, 57–60 (2011).
34. T. Hornung, M. Steiner, and P. Nitz, "Estimation of the Influence of Fresnel Lens Temperature on Energy Generation of a Concentrator Photovoltaic System," *Sol. Energy Mater. Sol. Cells* **99**, 333–338 (2012).
35. T. Schult, M. Neubauer, Y. Bessler, P. Nitz, and A. Gombert, "Temperature Dependence of Fresnel Lenses for Concentrating Photovoltaics," *2nd International Workshop on Concentrating Photovoltaic Optics and Power* (2009).
36. I. García, M. Victoria, and I. Antón, "Temperature Effects on CPV Solar Cells, Optics and Modules," in *Handbook of Concentrator Photovoltaic Technology*, (Wiley, 2016), pp. 481–564.
37. M. Victoria, R. Herrero, C. Domínguez, I. Antón, S. Askins, and G. Sala, "Characterization of the spatial distribution of irradiance and spectrum in concentrating photovoltaic systems and their effect on multi-junction solar cells," *Prog. Photovoltaics* **21**, 308–318 (2013).
38. C. Domínguez, I. Antón, G. Sala, and S. Askins, "Current-matching estimation for multijunction cells within a CPV module by means of component cells: Current-matching estimation for MJ cells within a concentrator," *Prog. Photovoltaics* **21**(7), 1478–1488 (2013).
39. S. R. Kurtz and M. J. O'Neill, "Estimating and controlling chromatic aberration losses for two-junction, two-terminal devices in refractive concentrator systems," in *Conference Record of the Twenty Fifth IEEE Photovoltaic Specialists Conference - 1996*, (1996), pp. 361–364.
40. P. Espinet-González, I. Rey-Stolle, C. Algora, and I. García, "Analysis of the behavior of multijunction solar cells under high irradiance Gaussian light profiles showing chromatic aberration with emphasis on tunnel junction performance: Analysis of the behavior of multijunction solar cells under Gaussian light profiles," *Prog. Photovoltaics* **23**, 743–753 (2015).
41. V. D. Rumyantsev, N. Y. Davidyuk, E. A. Ionova, P. V. Pokrovskiy, N. A. Sadchikov, and V. M. Andreev, "Thermal Regimes of Fresnel Lenses and Cells in "All-Glass" HCPV Modules," *AIP Conf. Proc.* **1277**, 89–92 (2010).
42. T. Hornung, A. Bachmaier, P. Nitz, and A. Gombert, "Temperature and wavelength dependent measurement and simulation of Fresnel lenses for concentrating photovoltaics," in *Photonics for Solar Energy Systems III*, vol. 7725 (International Society for Optics and Photonics, 2010), p. 77250A.
43. A. W. Bett, C. Baur, D. Frank, G. Lange, M. Meusel, S. van Riesen, G. Siefert, V. M. Andreev, and V. D. Rumyantsev, "FLATCON™-Modules. Technology and Characterisation," in *3rd World Conference on Photovoltaic Energy Conversion.*, (WCPEC-3 Organizing Committee, 2003).
44. M. Wiesenfarth, M. Steiner, T. Dörsam, G. Siefert, F. Dimroth, P. Nitz, and A. W. Bett, "FLATCON® CPV module technology: A new design based on the evaluation of 10 years of outdoor measurement data," in *15th International Conference on Concentrator Photovoltaic Systems (CPV-15)*, (Fes, Morocco, 2019), p. 030007.